

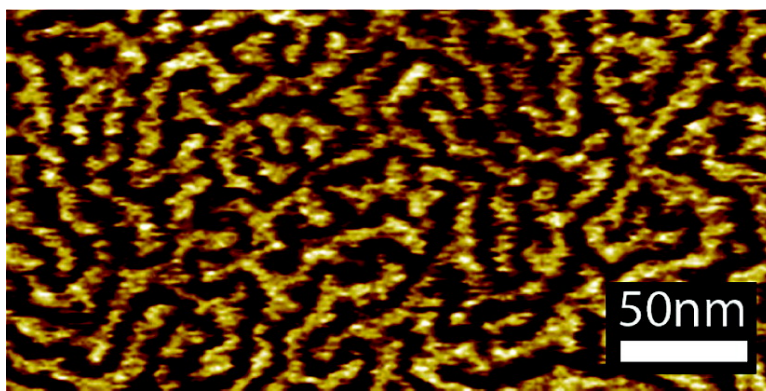
Note

Nonplanar Surface Organization of Monodendrons in Side-Chain Modified Liquid Crystalline Block Copolymers.

E. Sivaniah, J. Genzer, A. Hexemer, E. J. Kramer, M. L. Xiang, X. F. Li, C. K. Ober, and S. Magonov

Macromolecules, **2008**, 41 (24), 9940-9945 • DOI: 10.1021/ma8015097 • Publication Date (Web): 14 November 2008

Downloaded from <http://pubs.acs.org> on January 14, 2009



More About This Article

Additional resources and features associated with this article are available within the HTML version:

- Supporting Information
- Access to high resolution figures
- Links to articles and content related to this article
- Copyright permission to reproduce figures and/or text from this article

[View the Full Text HTML](#)



ACS Publications
High quality. High impact.

Macromolecules is published by the American Chemical Society, 1155 Sixteenth Street N.W., Washington, DC 20036

Nonplanar Surface Organization of Monodendrons in Side-Chain Modified Liquid Crystalline Block Copolymers.

E. Sivaniah,[†] J. Genzer,^{*} A. Hexemer,[§] and E. J. Kramer^{*}

Departments of Materials and Chemical Engineering,
UCSB, Santa Barbara, California 93106-5050

M. L. Xiang,[⊥] X. F. Li,^{||} and C. K. Ober^{*}

Materials Science and Engineering Department,
Cornell University, Ithaca, New York 14853-1501

S. Magonov[#]

Digital Instruments, Santa Barbara, California 93106

Received July 7, 2008

Revised Manuscript Received October 10, 2008

ABSTRACT: Scanning force microscopy (SFM) is used to investigate the surface structures of diblock copolymers of poly(styrene)-*block*-poly(isoprene) where a portion of the isoprene segments were modified to contain a semifluorinated alkane monodendron side group. The monodendrons consisted of either a single, double or triple attachment of the liquid crystalline mesogen group, $[-(\text{CH}_2)_p-(\text{CF}_2)_q\text{F}]$. Previously we reported that the surfaces of thin films of these materials contained small (~ 20 – 30 nm) dome-like structures that were independent of the coincident block copolymer microphase architecture. We show here that these surface features can also assume a worm-like structure depending on the composition of the monodendron. Furthermore thermal studies of the block copolymer and the isolated monodendron molecule using *in situ* SFM studies confirm the liquid crystalline origin of the surface structures.

Introduction

The chemical functionalization of polymers by fluorine based moieties has received much attention recently.^{1,2} From a technological point of view, these materials have desired superhydrophobic properties and can form protective coatings in applications from boat hulls to hard disk media.^{3,4} Fluoropolymers are also increasingly studied as potential materials for advanced technology applications, e.g. as photoresists.^{5,6}

In past studies the Ober group at Cornell University together with the Kramer group at UCSB have extensively explored the material properties of a combination of semifluorinated liquid crystalline mesogenic side groups with an amorphous polymer backbone.^{7–10} In doing so, the low surface energy properties of the fluorinated groups, the smectic self-assembling nature of the mesogens and the elastomeric properties associated with the polymer backbone have resulted in a hydrophobic coating

material with good thermal and mechanical stability and strong resistance to surface reconstruction.¹¹ Generically, we have used a semifluorinated alkane mesogenic group with the general formula $-(\text{CH}_2)_p-(\text{CF}_2)_q\text{F}$. These mesogens were attached as sidechains to the isoprene portion of a poly(styrene)-*block*-poly(isoprene) block copolymer (PS-*b*-PI). Several parameters within our physical system were variously investigated for their effect on the bulk and surface properties of the modified polymer. These parameters, including the relative and total length of the PS and PI blocks in the modified copolymer, the structure of the semifluorinated alkane mesogen (i.e., p , q), and the degree of attachment of the mesogen to the polymer backbone, provide a rich experimental landscape to explore.

A novel phenomenon was found to occur when three mesogenic groups were attached to a single node to form a monodendron that was subsequently used to modify the block copolymer.⁹ Dome-like surface structures (~ 20 nm) were formed on the polymer surface in a manner independent of the larger microphase structure from the block copolymer.⁸ It was proposed that the dome structures arose from a particular organization of the mesogenic groups at the surface arising from packing constraints. Analogous packing features within the interior of the material were not observed making this a surface specific phenomenon. This behavior is quite different to other supra-molecular organization seen in large dendritic molecules where nonsurface specific columnar or spherical meso-phases are reported through the organization of a dendritic side chain.^{12–14}

The dome structures we have observed are an example of nonplanar surface smectic organization. In this paper, we examine this organization further by altering the structural composition of the monodendrons. Moreover we confirm that the organizing principle arises from mesogenic packing effects by examination of the thermal stability of these surface structures.

Experimental Section

The modified poly(styrene)-*block*-poly(1,2-/3,4-isoprene) block copolymer studied here are referred to by the following general abbreviation, $\text{BC-}f\text{-DI.ArF}_q\text{H}_p$, where f represents the volume fraction of PS in the modified block copolymer. The attachment ratio, ar , is the fraction of isoprene repeat units that possess a modified sidegroup; the dendritic index, DI , represents the number of semifluorinated alkane mesogens that are attached to a modified isoprene unit. F_qH_p indicates that p CH_2 and q CF_2 groups are found on the mesogen itself. Polymers with DI values of 2 and 3 were synthesized by Xiang et al. and $DI = 1$ polymers prepared by Wang et al. (see Scheme 1).^{9,15} Due to a different synthetic route, the two and three-armed mesogenic side groups structures are more extended than $DI = 1$ side group. The main characteristics of the block copolymers discussed in this study are summarized in Table 1.

Samples were prepared by spin-casting solutions of the block copolymers in α - α - α -trifluorotoluene. Films of thickness ~ 150 – 300 nm were annealed at 150 °C at ultrahigh vacuum (10^{-8} Torr) for an hour and slowly cooled to room temperature to improve the quality of the final surface structure. The films were analyzed at room temperature with tapping mode scanning force microscopy (SFM) (Multimode III; Digital Instruments, Santa Barbara, CA). Additional SFM experiments were conducted *in situ* at elevated temperatures using a commercial adaptation of the multimode SFM hardware to include a heating stage. A description of this heating device may be found elsewhere.^{16,17} Typical operation parameters

^{*} To whom correspondence should be addressed.

[†] Present address: Cavendish Laboratory, Cambridge University, Cambridge CB3 0HE, U.K.

[§] Present address: Chemical Engineering Department, North Carolina State University, 911 Partners Way, Raleigh, NC 27695.

[⊥] Present address: Lawrence Berkeley National Laboratory, 1 Cyclotron Road Mail Stop 80 R0114, Berkeley, CA 94720-8229.

^{||} Present address: Nirooyal Chemical Company, 280 Elm St., Bldg 310, Naugatuck, CT 06770.

[#] Present address: Celgard LLC, 13800 South Lakes Dr. Charlotte, NC 28273.

^{*} Present address: Agilent Technology, 4330W Chandler Blvd, Chandler, AZ 85226.

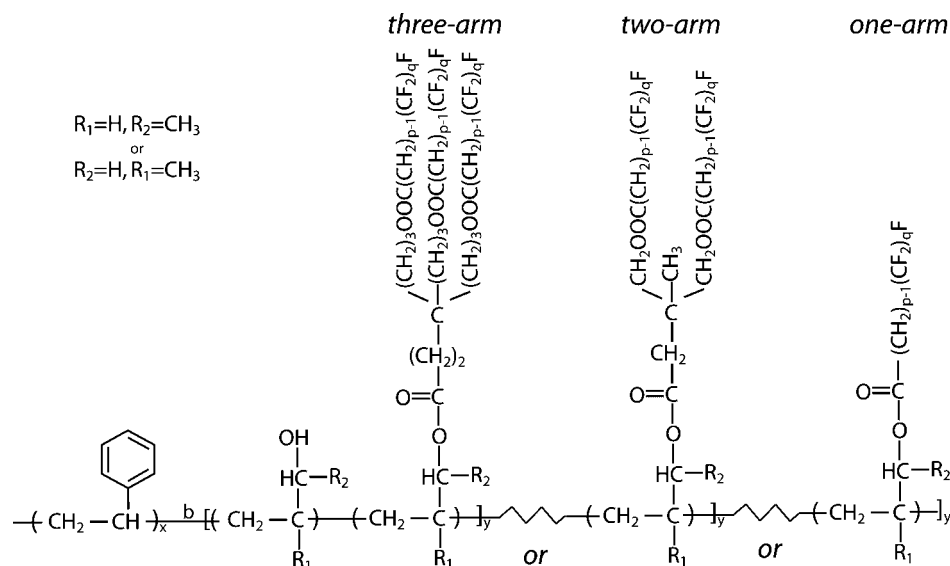
Scheme 1. Generic Chemical Structure of Block Copolymer Used in This Study (Adapted from Xiang et al.⁹)

Table 1. Chemical Structure and Surface Smectic Topology of Block Copolymers Used in This Study

| sample id | PS/PILC mol wt | attach. ratio | <i>f</i> | DI; <i>p</i> ; <i>q</i> | LC surface type |
|--|-------------------|------------------|----------|-------------------------|--------------------|
| BC _{0.26-3A_{0.53}F8H10} | 38.2K/107.1K | 0.531 | 0.26 | 3; 10; 8 | dome |
| BC _{0.25-3A_{0.58}F8H10} | 38.2K/114.9K | 0.585 | 0.25 | 3; 10; 8 | dome |
| BC _{0.21-3A_{0.73}F8H10} | 38.2K/141.9K | 0.733 | 0.21 | 3; 10; 8 | dome |
| BC _{0.42-3A_{0.56}F8H10} | 66.0K/90.9K | 0.562 | 0.42 | 3; 10; 8 | dome |
| BC _{0.54-3A_{0.58}F8H10} | 117K/101.6K | 0.587 | 0.54 | 3; 10; 8 | dome |
| BC _{0.72-3A_{0.42}F8H10} | 215K/79.9K | 0.420 | 0.72 | 3; 10; 8 | dome |
| BC _{0.31-2A_{0.68}F8H6} | 41.1K/93.4K | 0.683 | 0.31 | 2; 6; 8 | dome |
| BC _{0.33-2A_{0.58}F8H6} | 41.1K/80.8K | 0.581 | 0.33 | 2; 6; 8 | dome |
| BC _{0.32-2A_{0.62}F8H6} | 41.1K/86.0K | 0.623 | 0.32 | 2; 6; 8 | dome |
| BC _{0.41-2A_{0.68}F8H6} | 38.2K/85.4K | 0.680 | 0.41 | 2; 6; 8 | dome |
| BC _{0.26-2A_{0.78}F8H10} | 38.2K/105.4K | 0.781 | 0.26 | 2; 10; 8 | worm-like |
| BC _{0.29-2A_{0.66}F8H10} | 41.1K/98.9K | 0.663 | 0.29 | 2; 10; 8 | worm-like |
| BC _{0.42-2A_{0.34}F8H10} | 38.2K/51.2K | 0.344 | 0.42 | 2; 10; 8 | worm-like |
| BC _{0.41-2A_{0.37}F8H10} | 38.2K/54.9K | 0.374 | 0.41 | 2; 10; 8 | worm-like |
| BC _{0.45-1A_{1.00}F6H10} | 41.1K/59.9K | 1.00 | 0.45 | 1; 10; 6 | worm-like |
| BC _{0.42-1A_{1.00}F8H10} | 41.1K/70.6K | 1.00 | 0.42 | 1; 10; 8 | worm-like |
| BC _{0.39-1A_{1.00}F10H10} | 41.1K/84.7K | 1.00 | 0.39 | 1; 10; 10 | none |

were as follows: All scans were operated in the repulsive regime of the tip-sample interaction and under 'light' tapping conditions, where the ratio of the contact set point amplitude to the free oscillation amplitude was ~ 0.75 . A silicon nitride cantilever tip (of natural frequency ~ 160 Hz) was employed for all the SFM data collected. For heating measurements, the sample was placed on the heating stage at 30°C and allowed to equilibrate to eliminate imaging artifacts due to non-uniform thermal expansion of the sample and microscope components. The sample temperature was raised in increments of three or five degrees during which the SFM tip was withdrawn from the sample and between which SFM images were collected. The sample temperature reached the desired value in a matter of seconds with minimal overshooting by the thermo-controller of the heating stage.

Results and Discussion

Figure 1 shows the surface topology of five representative modified block copolymers (BCP) where the composition of the attached monodendron is varied. In considering the structures in this figure one must disregard the block copolymer microphase separating structure (e.g., the larger sinuous structure seen in Figure 1b or the larger spherical topography seen in Figure 1e).

In Figure 1a, a domelike surface structure is observed for BCPs with three-armed monodendrons containing $-(\text{CH}_2)_{10}-$

$(\text{CF}_2)_8\text{F}$ mesogens (as reported by Sivanian et al.⁸). The same domelike structures are found in BCPs with two-armed monodendrons of $-(\text{CH}_2)_6-(\text{CF}_2)_8\text{F}$ mesogens (Figure 1b). However the surface structure becomes worm-like in BCPs where the two-armed monodendrons contain mesogens with longer alkane groups, $-(\text{CH}_2)_{10}-(\text{CF}_2)_8\text{F}$, (Figure 1c) or in BCPs where there is a single mesogen $-(\text{CH}_2)_{10}-(\text{CF}_2)_6\text{F}$ in the modified isoprene repeat unit (Figure 1d). Although less distinct and of a finer scale (Figure 1e), these worm-like morphological features also occur when the single mesogen alkane structure is $-(\text{CH}_2)_{10}-(\text{CF}_2)_8\text{F}$. These smaller scale structures (typical lateral size of ~ 14 nm) are stable under SFM imaging and should not be confused with the smectic layer structures (~ 4 nm).

The attachment of mesogens to a single node leads to a splayed monodendron. We have argued in an earlier work that the dome-like surface structures arise from a competition between the molecular packing of these splayed monodendrons and the thin film surface tension. It is likely that this unique, surface specific, packing could be a function of the attachment ratio of modified side groups to the block copolymer, *ar*, the dendritic index, DI, and the makeup of the semifluorinated alkane itself, *p* and *q*.

As summarized in Table 1, three of the reported monodendron structures, F₈H₆ (2-armed) and F₈H₁₀ (2-armed and 3-armed) were attached to the PS-PI BCP with a series of different attachment ratios ranging from 0.35 to 0.78. The principal effect was to increase the relative volume fraction of the fluorinated isoprene phase and thus alter the larger microphase separated architecture. There was no discernible effect of *ar* on the architecture of the smaller surface structures.

In a previous paper,¹⁸ we have shown that the dome like structures are possible even when the monodendron-modified block copolymers are added as a minority component surfactant.¹⁹ Even when there is insufficient polymer to form a complete monolayer, portions of the surface contained dome structures. It may even be possible that these dome structures could be produced when polymer chains are simply end-functionalized with semi fluorinated monodendrons. Thus it is arguable that attachment ratio is not an important factor.

On the other hand, the composition and architecture of the mesogen, characterized by DI, *p* and *q*, do have an effect.

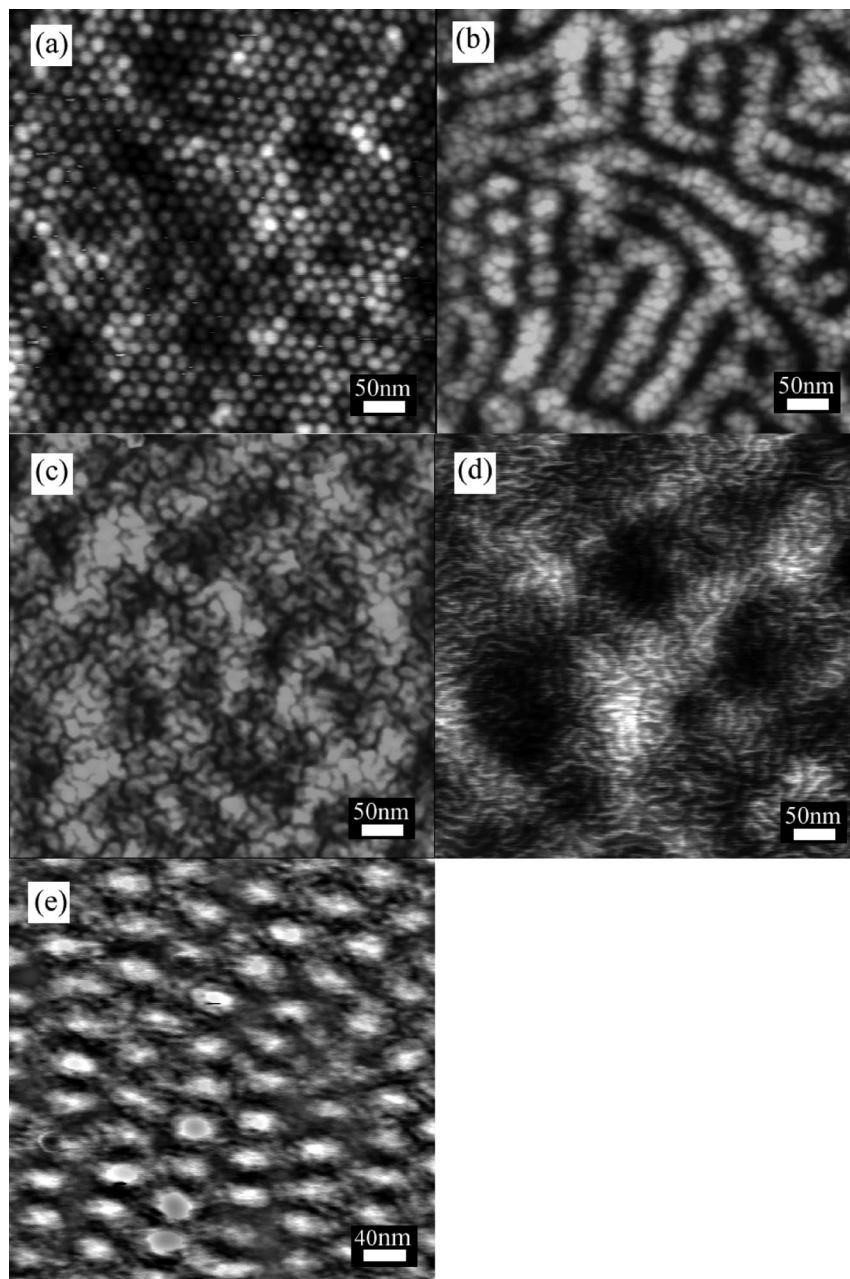


Figure 1. SFM images of various modified block copolymers. All images taken in height mode; (a) $\text{BC}_{0.54}\text{-3A}_{0.58}\text{F}_8\text{H}_{10}$ (Z gray scale, 0–5 nm); (b) $\text{BC}_{0.32}\text{-2A}_{0.62}\text{F}_8\text{H}_6$ (Z gray scale, 0–17 nm); (c) $\text{BC}_{0.41}\text{-2A}_{0.37}\text{F}_8\text{H}_{10}$ (Z gray scale, 0–5 nm); (d) $\text{BC}_{0.45}\text{-1A}_{1.00}\text{F}_6\text{H}_{10}$ (Z gray scale, 0–10 nm); (e) $\text{BC}_{0.42}\text{-1A}_{1.00}\text{F}_8\text{H}_{10}$ (Z gray scale, 0–3 nm).

Consider BCPs with a single mesogen in the side group. As summarized in Table 1, and seen in Figure 1, parts d and e, the worm-like structure becomes less distinct as the fluorinated segment increases in length from six to eight CF_2 groups. When there are ten CF_2 groups present in the mesogen, no surface structures are observed. This may correspond to a scenario where tightly packed fluorinated segments leading to an unbuckled, fluorinated top layer for the BCP containing $\text{F}_{10}\text{H}_{10}$ mesogens.

Within the bulk phase, the smectics are reported to exist as layers that are perpendicular to the bulk block copolymer interface.⁹ However near the polymer/air surface the surface smectic layer is arranged so that the terminal CF_3 groups homogeneously wet that interface.¹⁰ The dome and worm-like structures that we observe arise from a unique set of circumstances for the surface smectic layer. Specifically molecular splay in the monodendrons hinders perfect packing onto a flat monolayer surface. This is improved by allowing the monolayer

surface to buckle to form domes and worm-like surface features. The lateral dimensions of these latter structures is governed by a balance of an increased surface area for larger dome (or worm) structures and increased defect line length for smaller dome structures. A detailed treatment of this phenomenon is given in an earlier paper.⁸ As far as we know these structures are unique and rely on the ability of the isoprene backbone to accommodate the deformation of the surface smectic monolayer. A similar topographical phenomena might be expected in self-assembled monolayers of semifluorinated alkanes provided the SAM substrates themselves were able to deform to accommodate the buckling of the monolayer surface. Our structures do have a striking similarity to those reported by the Stupp group using oligoisoprene–oligostyrene diblocks that are converted to a oligotriblock by the addition of a rod-like polymer.²⁰ There, monolayers of the triblocks form mushroom-like structures whereas thicker films are found to self-assemble to form lamellar

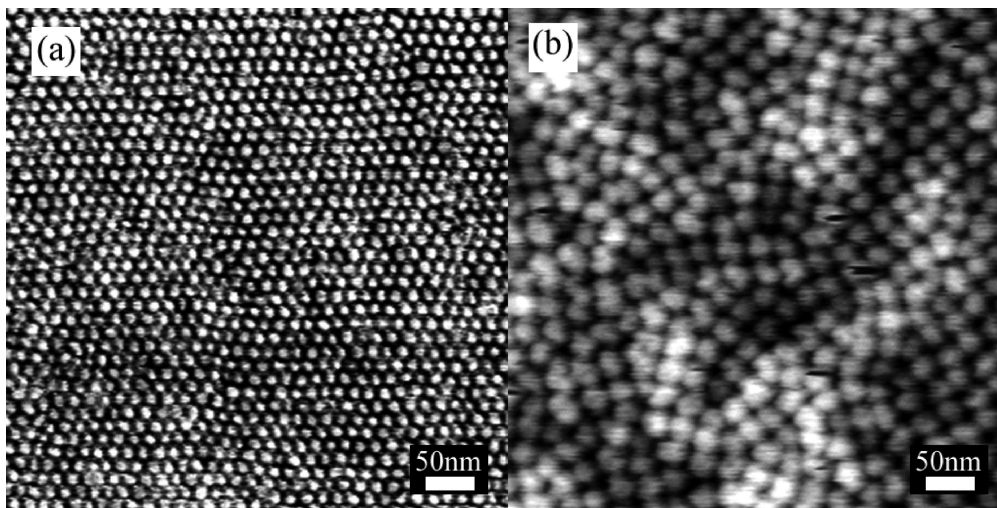


Figure 2. SFM images of unattached 3-armed $-(\text{CH}_2)_{10}-(\text{CF}_2)_8\text{F}$ mesogen: (a) after preparation by solvent casting; in SFM phase mode; (b) after annealing to above $T_{\text{S-I}}$ and slow cooling to room temperature, in SFM height mode (Z gray scale, 0–10 nm).

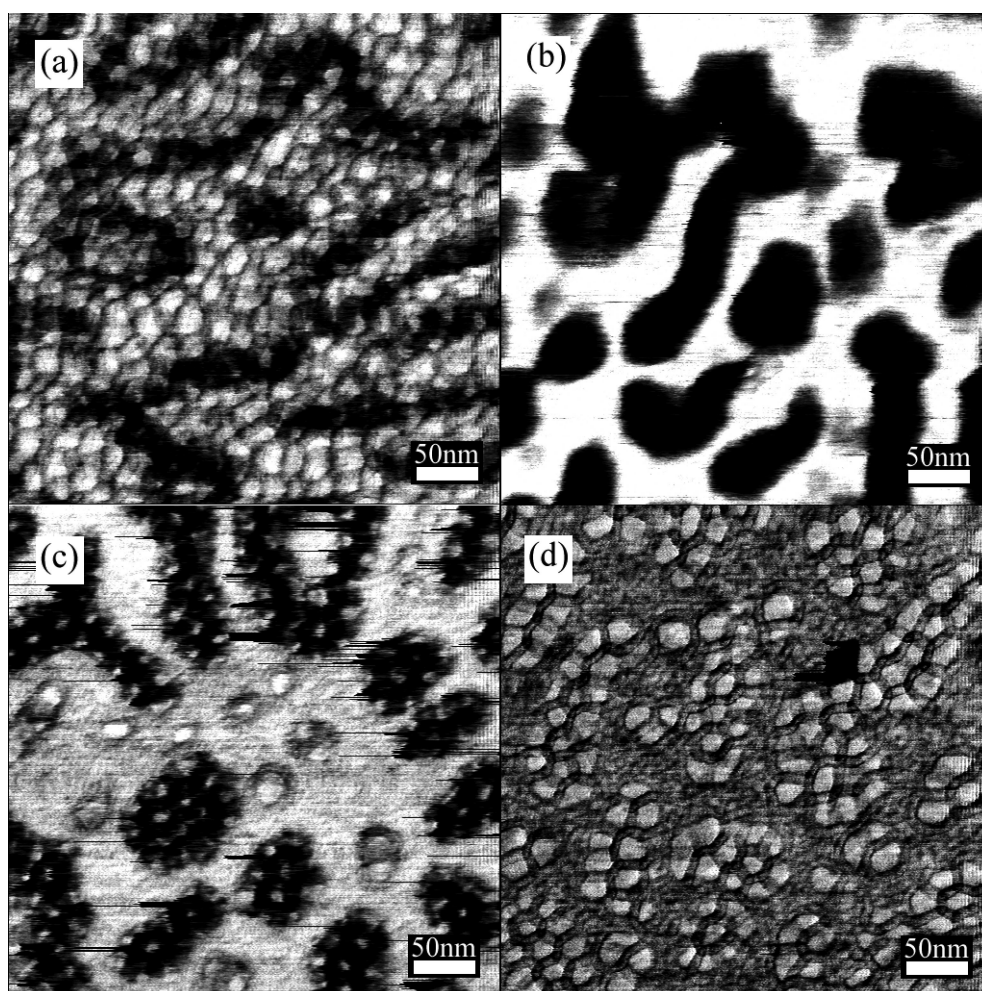


Figure 3. Phase mode SFM images of $\text{BC}_{0.42}\text{-}3\text{A}_{0.56}\text{F}_8\text{H}_{10}$ taken at different temperatures during heating and cooling cycle. (a) 60 °C; (b) 75 °C; (c) 55 °C; (d) 30 °C.

sheets. In our work, the observed dome and worm-like structures, were not detected in the smectic layers within the bulk of the material.

The three armed monodendron has a splayed conformation in three dimensions that is characterized by a solid angle. This three armed monodendron results in dome-like superstructures.

However such dome structures are also possible from two armed monodendrons (of F_8H_6) where the splayed conformation can be characterized by a simple angle. Whether the spatial distribution of molecular splay dictates the final superstructure architecture is not clear. Increasing the length of the hydrogenated alkane spacer in 2-armed mesogens from F_8H_6 to F_8H_{10}

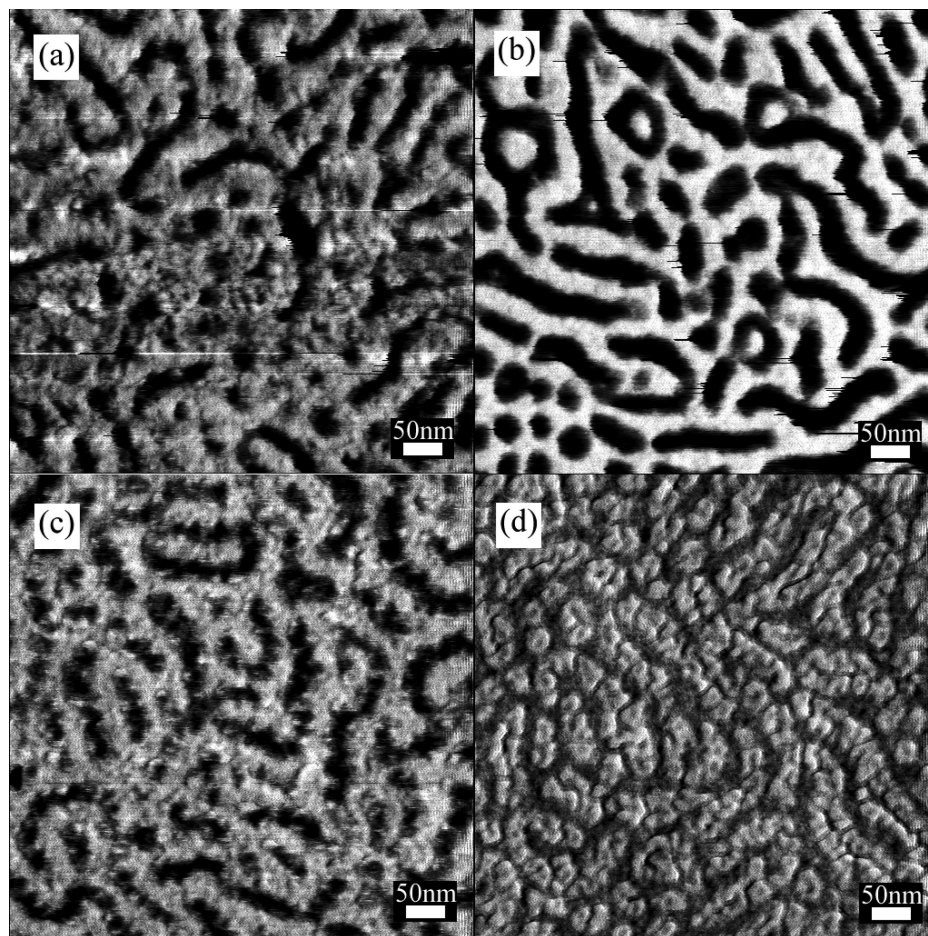


Figure 4. Phase mode SFM images of $\text{BC}_{0.42}\text{-2A}_{0.34}\text{F}_8\text{H}_{10}$ taken at different temperatures during heating and cooling cycle. (a) 51 °C; (b) 63 °C; (c) 48 °C; (d) 30 °C.

will reduce the molecular splay of the monodendron. In this case, this change leads to the formation of a worm-like structure. Equally, the worm-like structures are present in polymers containing single armed mesogens.

At present there is no indication whether a single function of DI, p and q determines whether the final structure will be worm-like or dome-like. However one may appreciate that increasing DI increases the effective tension experienced by each of the arms as the mesogen tries to pack onto a flat air surface. This tension is subsequently alleviated by packing the mesogens into nonplanar topographies. Similarly one expects that increasing the p/q ratio will decrease this tension effect. It may be that an intermediate decrease in overall ‘tension’ in the mesogen is responsible for the loss of curvature in the surface structures from the hemispherical (dome) domains to the cylindrical (worm-like) domains to a flat unbuckled surface (e.g., $\text{BC}_{0.39}\text{-1A}_{1.00}\text{F10H10}$ case). A similar argument exists for the transition in micelle structure in surfactant and block copolymer systems. For surfactants, this is through the invocation of a critical packing shape that is a function of headgroup size and chain crowding.²¹ For polymer based block copolymers and amphiphiles, this is a balance of interfacial area per block copolymer chain and the relative amount of stretching and compression against an entropic force that asymmetrically sized chains experience in order to fill a planar interface.²²

We were able to demonstrate through two further experiments that the observed surface structures arise from the liquid crystalline nature of the monodendrons. In a first experiment we observed by SFM the surface structure of an *unattached*

three-armed $\text{-(CH}_2\text{)}_{10}\text{-(CF}_2\text{)}_8\text{F}$ monodendron (the chemical structure is labeled **13** as described in Xiang et al.). A thin film of this molecule was prepared by slow solvent casting from a trifluorotoluene solution onto a silicon substrate. The result was a surface containing highly organized, hexagonally packed, dome structures (see Figure 2a). However, the characteristic dome diameter in this case is 13 nm; this is significantly smaller than the domes observed when the same side group was attached to a block copolymer (e.g., Figure 1a). Annealing this sample above the bulk smectic to isotropic transition temperature (T_{S-I}) for the monodendron and subsequently slowly cooling it under ambient conditions leads to the formation of less organized dome structures. Pertinently these are *larger* dome structures (Figure 2b) than those observed in Figure 1a and contain both HCP and BCC type packing. This difference in dome structure could be related to a number of additional effects including differences in the ambient air composition during solvent evaporation and during annealing.

In a second observation, we looked, *in situ*, at the formation of the dome-like structures as the modified block copolymer (containing three-armed $\text{-(CH}_2\text{)}_{10}\text{-(CF}_2\text{)}_8\text{F}$ mesogens) was annealed about this monodendron’s bulk smectic to isotropic transition temperature ($T_{S-I} \sim 63.3$ °C) in a heating and cooling temperature schedule (Figure 3). As the sample was heated from room temperature to temperatures below 60 °C the surface morphology was relatively unaltered. At 60 °C (Figure 3a) the observed surface shows a disappearance of the dome structures in some areas of the image. These areas coincide with a large change in the phase value of the SFM cantilever and may

indicate the onset of surface melting. There appears to be a characteristic length scale associated with the loss of the dome structures. At higher temperatures (e.g., 75 °C in Figure 3b) the SFM image became more heterogeneous while the dome structures disappeared completely. Subsequent cooling of the samples led to a reappearance of the surface smectic structures at 55 °C (Figure 3c). At lower temperatures (e.g., 30 °C in Figure 3d) the surface was only partially covered with the buckling structures. Extended annealing at 30 °C did not improve this condition.

Significantly the observed assembly and disassembly of the dome structures occur at temperatures close to the bulk T_{S-I} value for this polymer, 63.3 °C obtained by DSC. A similar correspondence was observed in a block copolymer modified by two-armed $-(CH_2)_{10}-(CF_2)_8F$ side groups for which the DSC observed T_{S-I} was 43.3 °C. *In situ* thermal SFM studies (Figure 4) showed the disappearance of the sinuous structures and enhanced cantilever phase differences at 51 °C (Figure 4a) and the reappearance of the structures at 48 °C during cooling (Figure 4c).

In Figure 4, annealing above T_{S-I} (see Figure 4b) did not result in the extended melting effects observed in Figure 3. The BCP in Figure 3 has a lamellar microphase separated architecture arranged in a parallel thin film orientation; thus upon annealing above T_{S-I} the entire film becomes liquid like in the plane of the film. In Figure 4, the underlying BCP structure is that of a cylindrical BCP that can stiffen the polymer film both in the plane of and normal to the thin film during annealing.

Conclusions

In an earlier paper, we made the first report on nonplanar mesogen organization at the air interface of a smectic layer where dome-like surface structures were reported as a result of molecular packing frustration. Here we have shown that the same effects can also lead to alternative packing arrangements, notably a *worm-like* structure. The final shape of this surface structure depends on the parameters that affect the intrinsic shape of the monodendron group such as the number of mesogens attached to a repeat unit or the size of the hydrogenated or fluorinated alkanes. The features we observe are quite subtly altered by these parameters and may only be possible in systems that contain highly surface active components within the mesogen. However our results are appropriate to and applicable within the current climate of producing nanoscale surface features. One promising area of exploration is the exploitation of these surface structures for patterning nanoscale features.²³

Acknowledgment. Primary support for this work was provided by the U.S. Office of Naval Research through Award No. N00014-

02-1-0170 and the OSD SERDP Program with additional support from the National Science Foundation Polymer Program Awards DMR074539 and DMR0518785. We also acknowledge the use of the Central Facilities of the Materials Research Laboratory funded by the National Science Foundation under the MRSEC program (UCSB MRL, DMR-0520415).

References and Notes

- (1) Hirao, A.; Sugiyama, K.; Yokoyama, H. *Prog. Polym. Sci.* **2007**, *32*, 1393–1438.
- (2) Kang, E. T.; Zhang, Y. *Adv. Mater.* **2000**, *12*, 1481–1494.
- (3) Genzer, J.; Efimenko, K. *Biofouling* **2006**, *22*, 339–360.
- (4) Gudipati, C. S.; Greenlief, C. M.; Johnson, J. A.; Prayongpan, P.; Wooley, K. L. *J. Polym. Sci., Part A: Polym. Chem.* **2004**, *42*, 6193–6208.
- (5) Krishnan, S.; Kwark, Y. J.; Ober, C. K. *Chem. Record* **2004**, *4* (5), 315–330.
- (6) Maier, G. *Prog. Polym. Sci.* **2001**, *26* (1), 3–65.
- (7) Li, X. F.; Andruzzi, L.; Chiellini, E.; Galli, G.; Ober, C. K.; Hexemer, A.; Kramer, E. J.; Fischer, D. A. *Macromolecules* **2002**, *35*, 8078–8087.
- (8) Sivaniah, E.; Genzer, J.; Fredrickson, G. H.; Kramer, E. J.; Xiang, M.; Li, X.; Ober, C.; Magonov, S. *Langmuir* **2001**, *17*, 4342–4346.
- (9) Xiang, M. L.; Li, X. F.; Ober, C. K.; Char, K.; Genzer, J.; Sivaniah, E.; Kramer, E. J.; Fischer, D. A. *Macromolecules* **2000**, *33*, 6106–6119.
- (10) Genzer, J.; Sivaniah, E.; Kramer, E. J.; Wang, J. G.; Korner, H.; Xiang, M. L.; Char, K.; Ober, C. K.; DeKoven, B. M.; Bubeck, R. A.; Chaudhury, M. K.; Sambasivan, S.; Fischer, D. A. *Macromolecules* **2000**, *33*, 1882–1887.
- (11) Schmidt, D. L.; Brady, R. F.; Lam, K.; Schmidt, D. C.; Chaudhury, M. K. *Langmuir* **2004**, *20*, 2830–2836.
- (12) Dziezok, P.; Sheiko, S. S.; Fischer, K.; Schmidt, M.; Moller, M. *Angew. Chem., Int. Ed.* **1997**, *36*, 2812–2815.
- (13) Percec, V.; Ahn, C. H.; Ungar, G.; Yeardley, D. J. P.; Moller, M.; Sheiko, S. S. *Nature* **1998**, *391* (6663), 161–164.
- (14) Schluter, A. D.; Rabe, J. P. *Angew. Chem., Int. Ed.* **2000**, *39*, 864–883.
- (15) Wang, J. G.; Mao, G. P.; Ober, C. K.; Krammer, E. J. *Macromolecules* **1997**, *30*, 1906–1914.
- (16) Fasolka, M. J.; Mayes, A. M.; Magonov, S. N. *Ultramicroscopy* **2001**, *90* (1), 21–31.
- (17) Jiang, Y.; Jin, X. G.; Han, C. C.; Li, L.; Wang, Y.; Chan, C. M. *Langmuir* **2003**, *19*, 8010–8018.
- (18) Hexemer, A.; Sivaniah, E.; Kramer, E. J.; Xiang, M.; Li, X.; Fischer, A.; Ober, C. K. *J. Polym. Sci., Part B: Polym. Phys.* **2004**, *42*, 411–420.
- (19) Thompson, R. L.; Narrainen, A. P.; Eggleston, S. M.; Ansari, I. A.; Hutchings, L. R.; Clarke, N. J. *Appl. Polym. Sci.* **2007**, *105*, 623–628.
- (20) Stupp, S. I.; LeBonheur, V.; Walker, K.; Li, L. S.; Huggins, K. E.; Keser, M.; Amstutz, A. *Science* **1997**, *276* (5311), 384–389.
- (21) Israelachvili, J. N. *Intermolecular and Surface Forces*, 2nd ed.; Elsevier: Amsterdam, 1991.
- (22) Hamley, I. W. *The Physics of Block Copolymers*; Oxford University Press: Oxford, U.K., 1998.
- (23) Huck, W. T. S. *Angew. Chem., Int. Ed.* **2007**, *46*, 2754–2757.

MA8015097